Hindawi Publishing Corporation
ISRN Nanomaterials
Volume 2014, Article ID 612154, 9 pages
http://dx.doi.org/10.1155/2014/612154

Research Article

Correlation between Structure and Dielectric Breakdown in LDPE/HDPE/Clay Nanocomposites

B. Zazoum, E. David, and A. D. Ngô

Department of Mechanical Engineering, École de Technologie Supérieure (ÉTS), 1100 Notre-Dame Street West, Montreal, QC, Canada H3C 1K3

Correspondence should be addressed to E. David; eric.david@etsmtl.ca

Received 7 January 2014; Accepted 3 March 2014; Published 19 March 2014

Academic Editors: M. Avella, J. Bai, J. W. Gilman, S.-R. Jian, and D. Ma

Cross-linked polyethylene (XLPE) is commonly used in medium/high voltage insulation due to its excellent dielectric properties and acceptable thermomechanical properties. To improve both electrical and thermal properties to a point that would possibly avoid the need for crosslinking, nanoclay fillers can be added to polymer matrix to form nanocomposites materials. In this paper, PE/clay nanocomposites were processed by mixing a commercially available premixed polyethylene/O-MMT masterbatch into a polyethylene blend matrix containing 80 wt% low density polyethylene LDPE and 20 wt% high density polyethylene HDPE with and without compatibilizer using a corotating twin-screw extruder. Various characterization techniques were employed in this paper, including optical microscopy, AFM, TEM, TGA, DMTA, and dielectric breakdown measurements in order to understand the correlation between structure and short-term dielectric breakdown strength.

1. Introduction

Polyethylene is the insulation dielectric material of choice because of its high dielectric strength coupled with low dielectric loss, in addition to lending itself to easy processing. Furthermore, this polymer can be extensively recycled, making it a suitable candidate for replacing its cross-linked counterpart, which has limited recyclability.

With conventional composite material, the filler is large or micrometric in size. It has been reported that adding microfiller has a negative effect on dielectric breakdown strength [1] due to the enhancement of the electric field around the aggregated filler particles, leading to decreased breakdown strength. To overcome these limitations, nanocomposite was used as an alternative to replace conventional composite [1–15]. Adding a nanoparticle to the polymer matrix resulted in a decrease in the internal electric field due to the reduction in particle size [16]. It has also been suggested that adding nanoclay can significantly decrease charge accumulation, which leads to increase in dielectric breakdown strength [17]. In nanocomposites, the interface between the nanoclay and the polymer matrix is very large, compared to that of composite or microcomposite materials. Several authors have reported that interface region plays an essential role in improving the insulating performance of nanodielectric materials [18–24].

In this paper, a blend of 80 wt% of LDPE and 20 wt% of HDPE was used as a matrix. The nanocomposite was prepared by melt-compounding the polymer matrix with nanoclay filler using a corotating twin-screw extruder.

Only a few studies have focused on the structure-dielectric breakdown correlation in polyethylene/clay nanocomposites [18]. To understand this relationship, microscopic observation, thermal behavior, and dynamic mechanical thermal analysis, as well as short-term dielectric breakdown, have been studied.

2. Experiment

2.1. Materials. Low density polyethylene LDPE (LF-Y819-A) with a melt flow index of 0.75 g/10 min and a density of 0.919 g/cm^3 was supplied by NOVA, Canada, while high density polyethylene HDPE (DGDP-6097 NT 7) with a melt flow index of 10.5 g/10 min and a density of 0.948 g/cm^3 was purchased from DOW, USA. The compatibilizer was

Table 1: Sample designation and formulation.

Sample designation	LLDPE (wt%)	LDPE/HDPE (wt%)	PE-MA (wt%)	O-MMT (wt%)
MB	50	—	—	50
PE	—	100	0	0
PE/O-MMT	5	90	0	5
PE/O-MMT/PE-MA	5	80	10	5

anhydride modified polyethylene PE-MA (Fusabond E226) with a melt flow index of 1.75 g/10 min and a density of 0.930 g/cm^3, supplied by DuPont Canada. A masterbatch of LLDPE/O-MMT (NanoMax) obtained from Nanocor containing 50 wt% of organomodified montmorillonite (O-MMT) and 50 wt% of linear low density polyethylene LLDPE.

2.2. Preparation of Nanocomposites. The LDPE, HDPE, PE-MA, and the LLDPE/O-MMT masterbatch were dried in a vacuum oven at 40°C for a minimum of 48 hours. Nanocomposites were prepared by melt-compounding using a corotating twin-screw extruder (Haake Polylab Rheomex OS PTW16, $D = 16$ mm, $L/D = 40$). The screw speed was set at 140 rpm and the feed rate was at 1 kg/h, while the hopper-to-die temperature profile was 170–180°C. The ingredients were manually premixed before being fed into the twin-screw extruder. After extrusion, the pellets were press-molded to form thin plates with a thickness of 590 μm using an electrically heated hydraulic press. The compositions and sample designations for the prepared nanocomposites are listed in Table 1.

3. Characterization and Measurements

3.1. Optical Microscopy. The morphological properties were carried out using an optical microscope (CE, NMM-800TRF) with a color camera (LEMEX) attached. Observations were realized at a lens magnification of 200x in transmission mode. All samples were prepared as a thin film with a thickness of 200 μm.

3.2. Atomic Force Microscopy (AFM). Microstructures of polyethylene/clay nanocomposites were evaluated using an atomic force microscope (DiNanoScope, Vecco, USA) in tapping mode. The images of the surface topography were then analysed using the Nanoscope (R) III software, version 5.30r.sr3. The nanoclay appeared brighter than the polyethylene matrix. Samples with a thickness of 590 μm were used, and all measurements were carried out at ambient conditions.

3.3. Transmission Electron Microscopy (TEM). The quality of dispersion of the nanoclays in the polymer matrix was examined by transmission electron microscope (TEM). Ultrathin sections with a thickness of 50–80 nm were cut from the molded plaque of PE/O-MMT and PE/O-MMT/PE-MA nanocomposites at −120°C using an ultramicrotome equipped with a diamond knife. The samples were then examined using a high resolution FEM Tecnai G2 F20 with accelerating voltage of 200 kV.

3.4. TGA Characterization. Thermogravimetric analysis (TGA) of PE and its nanocomposites was performed on a PYRIS Diamond TG-DTA. The heating process was executed from 50 to 700°C at a 10°C/min heating rate. All measurements were carried out under air and nitrogen atmosphere to evaluate the thermal oxidation and the thermal degradation of the materials, respectively. The nanoclay loading of the nanocomposites materials was also evaluated using this technique.

3.5. Dynamic Mechanical Analysis by DMTA. The thermomechanical properties of the neat PE blend and its nanocomposites were obtained using a dynamic mechanical thermal analysis (DMTA).

Dynamic stress σ and strain ε are given by

$$\sigma = \sigma_0 \sin(\omega t + \delta), \qquad \varepsilon = \varepsilon_0 \sin(\omega t), \tag{1}$$

where ω is the angular frequency and δ is the phase angle.

The complex modulus E^* is given by

$$E^* = E' + iE'', \tag{2}$$

where the real part E' reflects the elastic energy stored in the material. The imaginary part E'' describes the energy dissipated.

The loss factor $\tan\delta$ is the damping performance and is represented by

$$\tan\delta = \frac{E''}{E'}. \tag{3}$$

Rectangular geometry specimens with a 14 mm length, a 7 mm width, and a 1 mm thickness were used. All the specimens were cut from the compression-molded plaques. The measurements were carried out in dual cantilever mode at a fixed frequency of 1 Hz and a strain of 0.02%. The samples were clamped with a 20 cN·m torque in order to achieve reproducible results and were all cooled down with liquid nitrogen to −30°C and then kept for 10 minutes at that temperature.

Storage modulus E' and loss modulus E'' of PE and its nanocomposites were measured from −30 to 100°C at a 5°C/min heating rate. This slow heating rate was chosen in order to avoid having the material moving outside the thermodynamic equilibrium.

3.6. Dielectric Strength. The dielectric breakdown was measured according to the ASTM D 149 standard, using a BAUR

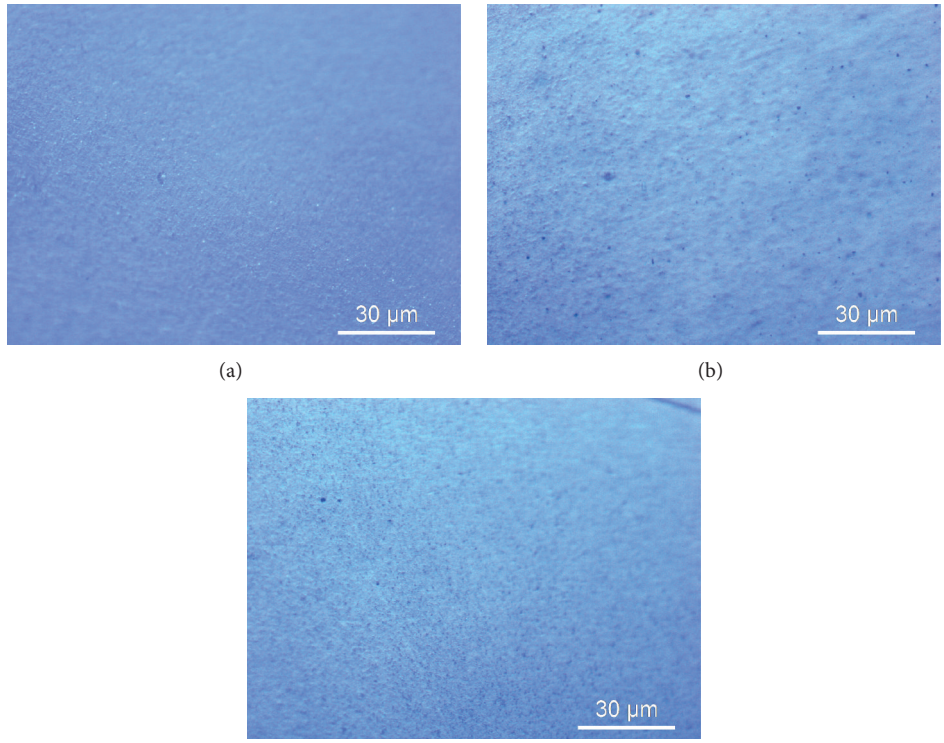

(a) (b) (c)

Figure 1: Optical microscope images of (a) neat PE, (b) PE/O-MMT, and (c) PE/O-MMT/PE-MA.

DTA 100 device to hold both the samples and the surrounding medium. A sample with an average thickness of 590 μm was immersed in a mineral oil (Voltesso 35, ESSO Imperial Oil) and placed between two spherical electrodes 12.5 mm in diameter. A 60 Hz voltage was raised at a rate of 2 kV/s from 0 V until the sample failed.

The dielectric strength E depends on the electrical voltage at breakdown V and thickness of specimen e:

$$E = \frac{V}{e}. \tag{4}$$

The dielectric strength data were processed using the two-parameter Weibull statistical distribution (Std-930, 2004). The Weibull statistical distribution in the case of two parameters can be written as

$$P(E) = 1 - \exp\left[-\left(\frac{E}{\alpha}\right)^{\beta}\right], \tag{5}$$

where P denotes the cumulative probability of electrical failure, E is the experimental dielectric strength, α is the scale parameter which represents the breakdown strength at the cumulative failure probability of 63.2%, and finally β is a shape parameter related to the scatter of data. According to the IEEE 930-2004 standard, the probability of failure $P(i, n)$ associated with the E_i data can be approximated by

$$P(i, n) = \frac{i - 0.44}{i + 0.25}, \tag{6}$$

where i is the ith result when the breakdown values are sorted in ascending order and n denotes the number of data points. For this work, $n = 20$.

The commonly used 90% confidence intervals were used to compare sets of data by verifying the overlapping of the confidence limits at the 63.2th percentile.

4. Results and Discussion

4.1. Optical Microscopy. Most studies have often used TEM to evaluate the quality of dispersion at high magnifications, while only few works have employed optical microscopy to investigate nanoclay morphologies at low magnifications [25]. The optical microscopy images of the polyethylene blend and its nanocomposites are shown in Figure 1. In the PE/O-MMT nanocomposites, the presence of significant aggregates with varied dimensions was observed (Figure 1(b)) which was not the case in the neat PE (Figure 1(a)). When the compatibilizer was added, the number and size of agglomerates were decreased (Figure 1(c)). This is due to the well-dispersed nanoclay platelet in the polyethylene matrix under the effect of processing conditions and compatibilizer.

4.2. Surface Roughness. In this paper, AFM height images of PE, PE/O-MMT, and PE/O-MMT/PE-MA were used in order to study the dispersion of nanoclay in the polymer matrix. The surface properties of neat PE and its two nanocomposites in 3D height image are shown in Figure 2. It can be seen that the surface of the neat PE (Figure 2(a))

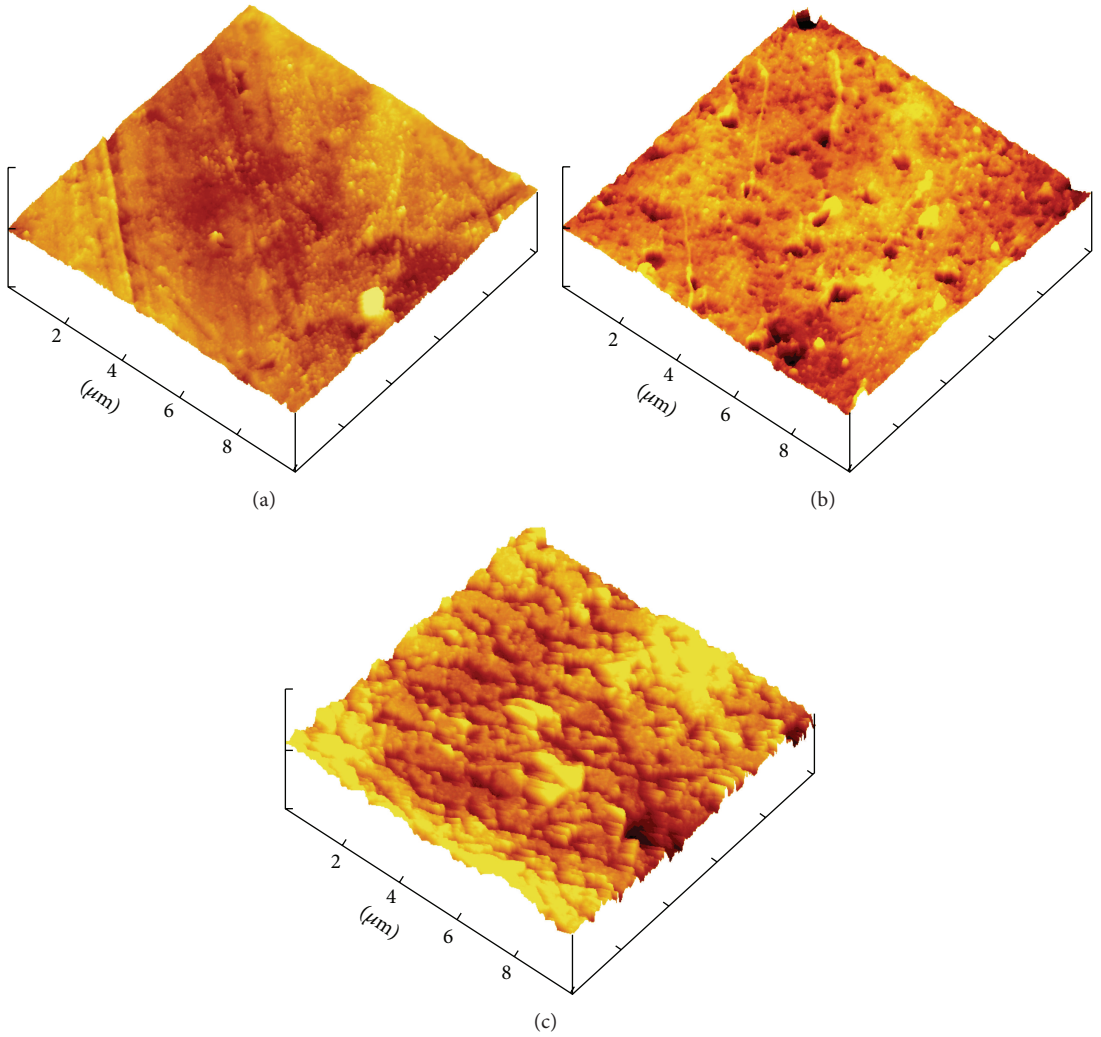

Figure 2: AFM height images of (a) neat PE, (b) PE/O-MMT, and (c) PE/O-MMT/PE-MA.

Table 2: Surface roughness data of PE and its nanocomposites.

Nanocomposites	R_a (average surface roughness) (nm)	R_q (root mean squared) (nm)
PE	11.0	16.3
PE/O-MMT	13.5	25.4
PE/O-MMT/PE-MA	11.7	18.0

is relatively smooth in comparison with those of PE/O-MMT (Figure 2(b)) and PE/O-MMT/PE-MA (Figure 2(c)) nanocomposites. From the surface roughness data depicted in Table 2, it is evident that PE/O-MMT/PE-MA shows a decrease in the root mean squared R_q and average surface roughness R_a values when compared with PE/O-MMT. The decrease in surface roughness can be attributed to a decrease in aggregate size [26]. From the images, it can also be seen that, in the compatibilized nanocomposites, the nanoclays are more oriented and structured on the surface. This is due to the good dispersion of nanoclay in PE/O-MMT/PE-MA nanocomposites [27].

4.3. Clay Dispersion by TEM. Because of the small size of the region examined by TEM, the description of the quality of dispersion was qualitative. TEM micrographs of PE/O-MMT and PE/O-MMT/PE-MA are shown in Figure 3. It can be seen that clay is presented as tactoids in the PE/O-MMT nanocomposites (Figure 3(a)). When the compatibilizer was added, the microstructure of the nanocomposites was presented as a combination of intercalated and exfoliated nanoclay layers (Figure 3(b)). A better dispersion of the clay platelets was achieved for PE/O-MMT/PE-MA than for the nanocomposites without a compatibilizer. This result is in agreement with our previous SEM and XRD measurements [28].

4.4. Thermal Properties. Figure 4 shows the TGA curves for neat PE and its nanocomposites PE/O-MMT and PE/O-MMT/PE-MA in air atmosphere. The thermal degradation

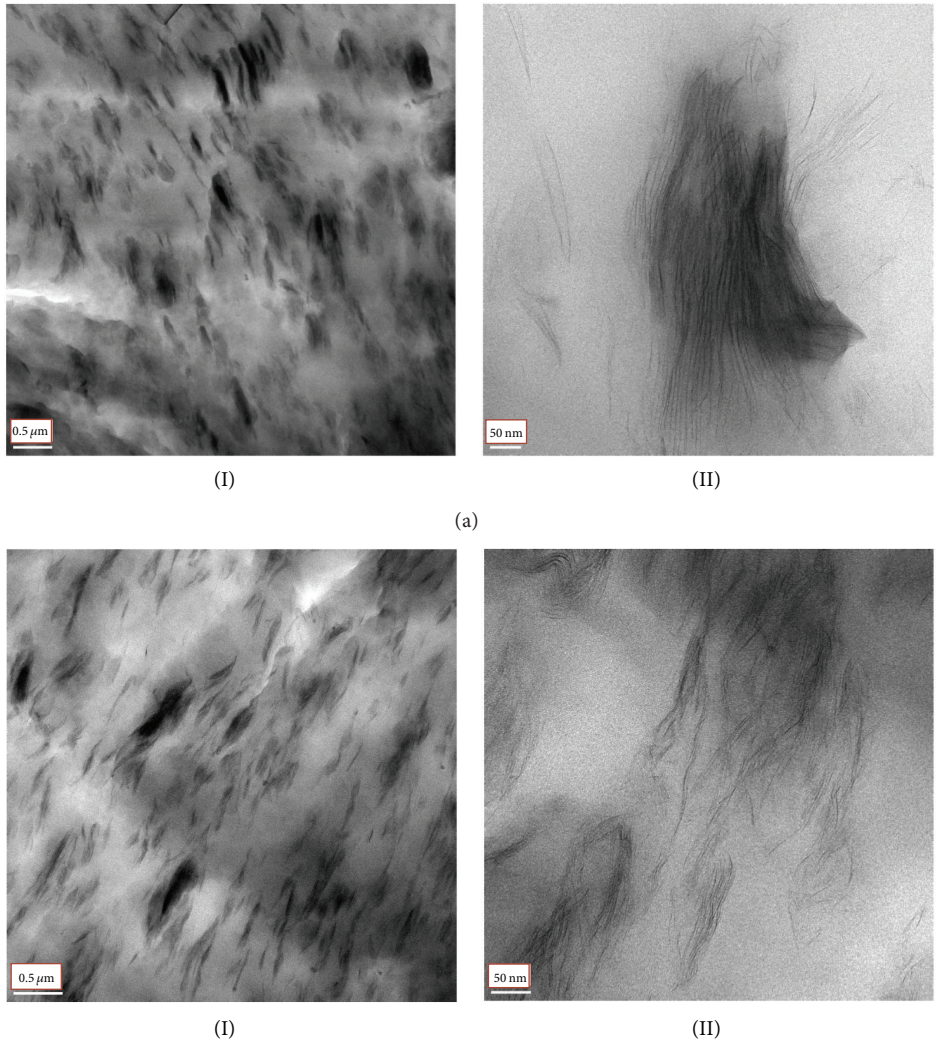

Figure 3: Low (I) and high (II) magnification TEM images of nanocomposites: (a) PE/O-MMT and (b) PE/O-MMT/PE-MA.

parameters derived from these curves are given in Table 3. It is apparent from these results that the initial degradation temperatures for both nanocomposites are higher than for the neat PE. For PE/O-MMT/PE-MA the decomposition temperatures $T_{10\%}$ and $T_{50\%}$ at 10% and 50% weight loss, respectively, of these compatibilized nanocomposites were slightly higher than the PE/O-MMT nanocomposites. This improvement can be due to maleic anhydride polyethylene. It has been reported [29] that, in the presence of this kind of compatibilizer, more intercalation/exfoliated layers can be formed in the polymer matrix and that there is an improvement in the barrier action for diffusion of oxygen into the nanocomposites which can inhibit material decomposition in air.

The thermal scans of PE, PE/O-MMT, and PE/O-MMT/E226 nanocomposites in nitrogen atmosphere are shown in Figure 5, and the degradation temperatures as well as ash content are depicted in Table 4. These results show that the thermal stability of the nanocomposite materials is enhanced when compared to that of the neat PE. On the other hand, it can be seen that the TGA thermogram in

Table 3: TGA data of PE and its nanocomposites in air atmosphere.

Sample	$T_{10\%}$ (°C)	$T_{50\%}$ (°C)	Loading (wt%)
PE	389.38	430.00	0
PE/O-MMT	434.06	468.59	3.88
PE/O-MMT/PE-MA	440.16	471.63	3.89

Table 4: TGA data of PE and its nanocomposites in nitrogen atmosphere.

Sample	$T_{10\%}$ (°C)	$T_{50\%}$ (°C)	Loading (wt%)
PE	413.75	456.40	0
PE/O-MMT	446.25	464.53	3.42
PE/O-MMT/PE-MA	448.28	466.56	3.40

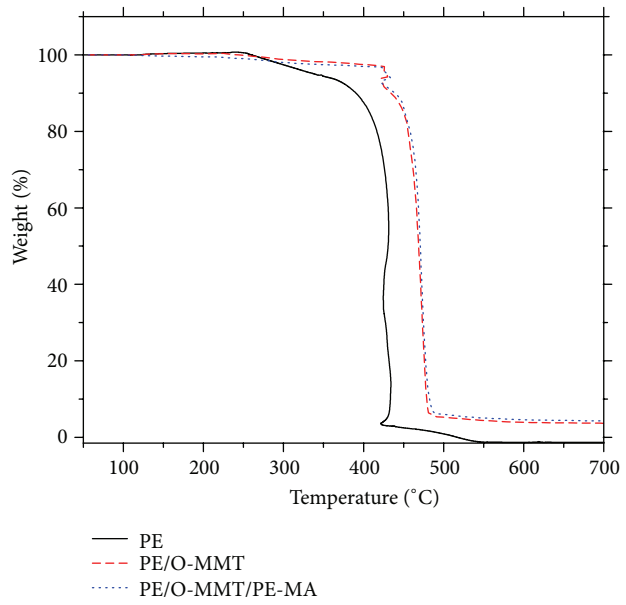

Figure 4: TGA decomposition curves of neat PE and its nanocomposites in air environment.

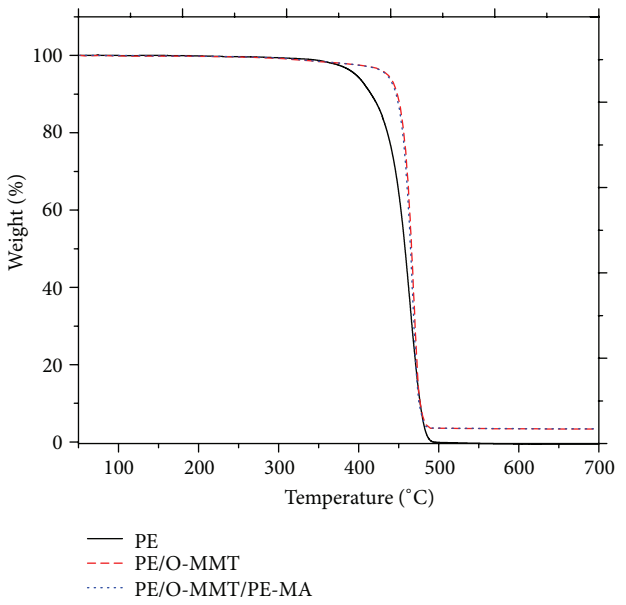

Figure 5: TGA decomposition curves of neat PE and its nanocomposites in a N_2 environment.

nitrogen atmosphere related to PE/O-MMT nanocomposites is superimposed over that of PE/O-MMT/PE-MA.

4.5. Dynamic Mechanical Behaviour. Thermomechanical analysis using DMTA was used to understand the evolution of the viscoelasticity of the nanocomposites over a wide range of temperatures. This technique provides better information on the quality of dispersion of the nanoclay filler in the polymer matrix [30, 31]. The storage modulus E' and loss modulus E'' curves of PE and its nanocomposites are depicted in Figures 6 and 7, which show the variation of storage and loss modulus, respectively, as a function of temperature. It is evident that the E' of neat PE and its nanocomposites decreases with an increase in temperature. This is due to the increase in the molecular motion of the polymer chains when the temperature increases. As depicted in Tables 5 and 6, it was found that the incorporated O-MMT improved the storage and loss modulus; at room temperature (25°C), the storage and loss moduli increased from 0.474 GPa and 0.054 GPa, respectively, in the neat PE blend to 0.561 GPa and 0.071 GPa, respectively, in the PE/O-MMT nanocomposites. This noticeable improvement in the thermomechanical stability of these nanocomposites materials from low to high temperatures was caused by the strong interactions between the interface of exfoliated/interacted nanoclay layers and the polymer matrix [32]. On the other hand, compatibilized nanocomposites showed slightly higher storage and loss moduli than nanocomposites without compatibilizers. These results clearly show that the storage modulus value is correlated with the quality of dispersion in nanocomposites materials [33].

4.6. Dielectric Breakdown Measurements. A typical image of a breakdown path for a PE/O-MMT sample in 2D and 3D

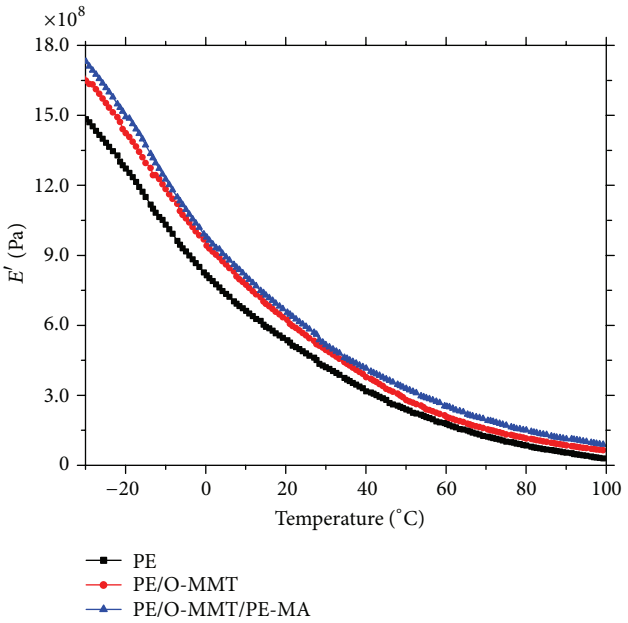

Figure 6: Storage modulus E' of neat PE, PE/O-MMT, and PE/O-MMT/PE-MA nanocomposites as a function of temperature at 1 Hz.

presentation is shown in Figures 8(a) and 8(b), respectively. Figure 9 shows the Weibull cumulative failure probability plot for the dielectric strength of pure PE and its nanocomposites. As reported in Table 7, for PE, PE/O-MMT, and PE/O-MMT/PE-MA, the scale parameters α were 70.3, 82.4, and 85.7 kV/mm, respectively, and the shape parameters β were 18.6, 13.2, and 10.8, respectively. It can clearly be observed from the scale parameter values α and from the confidence intervals that adding O-MMT to the polyethylene matrix

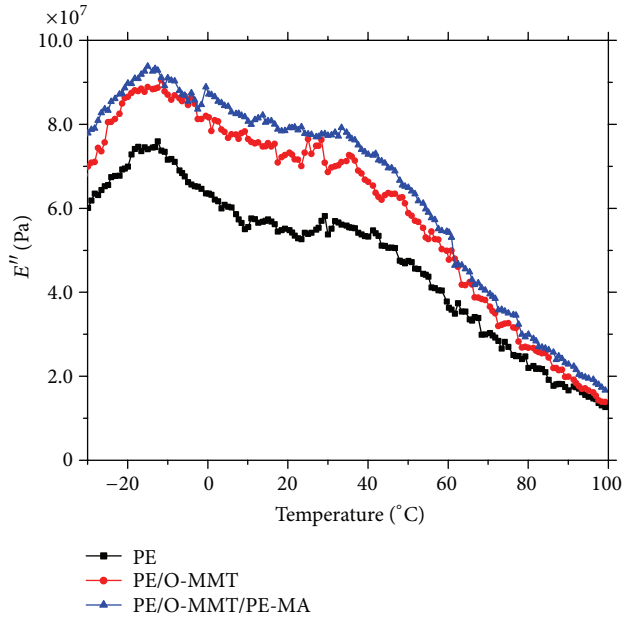

Figure 7: Loss modulus E'' of neat PE, PE/O-MMT, and PE/O-MMT/PE-MA nanocomposites as a function of temperature at 1 Hz.

Table 5: Effect of O-MMT clay and compatibilizer on storage modulus E' at different temperatures.

Samples	Storage modulus, E' (GPa)		
	−30°C	25°C	90°C
PE	1.485	0.474	0.051
PE/O-MMT	1.651	0.561	0.095
PE/O-MMT/PE-MA	1.725	0.594	0.117

Table 6: Effect of O-MMT clay and compatibilizer on loss modulus E'' at different temperatures.

Samples	Loss modulus, E'' (GPa)		
	−30°C	25°C	90°C
PE	0.060	0.054	0.017
PE/O-MMT	0.069	0.071	0.020
PE/O-MMT/PE-MA	0.076	0.077	0.023

leads to a noticeable increase in the material dielectric strength. This could be explained by the major role played by the interface between the PE matrix and the nanoclay particles, which could have an impact on the space charge distribution and charge densities. In turn, this probably led to a better distribution of the electrical stress [34]. When the compatibilizer was added to PE/O-MMT nanocomposites, a further improvement of the breakdown strength was noted. A possible explanation relates to the change of microstructure which occurred with the addition of the compatibilizer into the PE/O-MMT nanocomposites. This change of microstructure was already underlined by the microscopic observation results discussed above.

The shape parameter value β decreases when O-MMT is added to the PE matrix. With this parameter being an

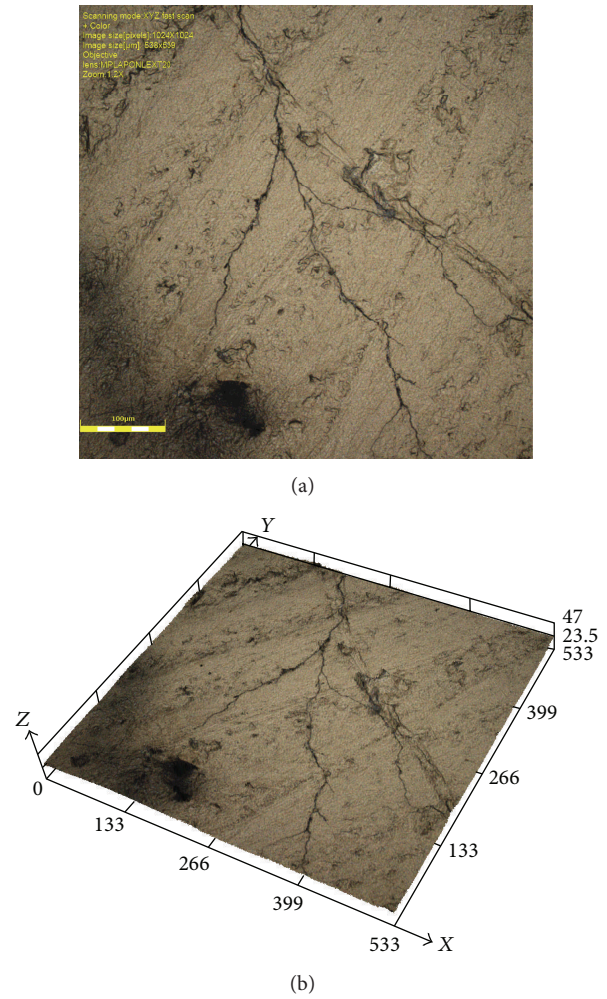

Figure 8: Typical breakdown path for PE/O-MMT in (a) 2D and (b) 3D visualizations, observed by high resolution optical microscope.

indication of the data's scattering, this could indicate either a nonuniform dispersion of the O-MMT or a partial exfoliation of the O-MMT [35].

5. Conclusion

A commercial nanoclay masterbatch was used in this study to prepare PE/clay nanocomposites. The effect of O-MMT clay and compatibilizer on the structure and dielectric breakdown behaviour in PE was investigated. Microstructure characterizations by microscopic observation revealed that nanoclay layers were more intercalated/exfoliated in PE/O-MMT/PE-MA than in PE/O-MMT, thanks to the presence of a compatibilizer. These results are in agreement with TGA and DMTA measurements. Dielectric strength measurements showed that, in PE/O-MMT nanocomposites, significant improvements in dielectric breakdown strength can be reached, as compared to neat PE. When the compatibilizer was added to PE/O-MMT nanocomposites, a further improvement in breakdown strength was noticed. This may suggest a correlation between morphology and breakdown strength

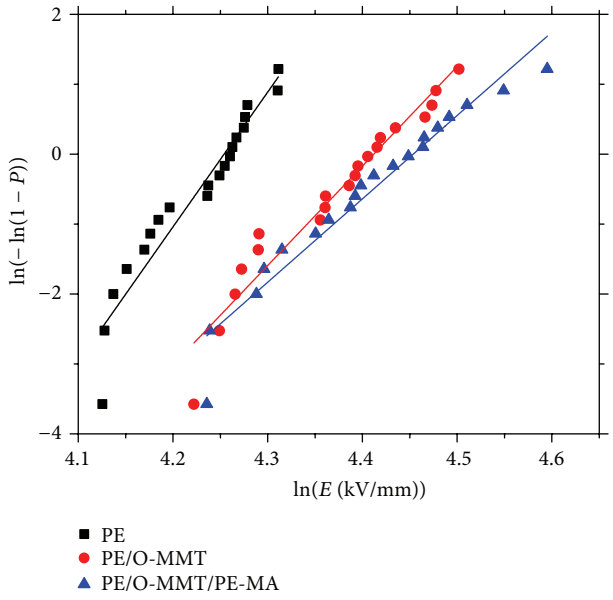

Figure 9: Weibull probability plot of dielectric strength of neat PE, PE/O-MMT, and PE/O-MMT/PE-MA.

Table 7: Weibull parameters for dielectric breakdown strength of PE and its nanocomposites.

Samples	α(kV/mm)	β	90% confidence intervals for α (kV/mm)
PE	70.3	18.6	(68.7, 71.7)
PE/O-MMT	82.4	13.2	(79.8, 84.7)
PE/O-MMT/PE-MA	85.7	10.8	(82.4, 88.7)

and that dielectric characterization, especially breakdown strength and dielectric response [28] measurements, can be exploited as an indirect technique for evaluating the degree of dispersion of nanoclay layers in polymer nanocomposites. Further studies will be necessary to confirm the results obtained.

Conflict of Interests

The authors declare that there is no conflict of interests regarding the publication of this paper.

Acknowledgments

The authors are grateful for the financial support from the National Sciences and Engineering Research Council of Canada (NSERC). TEM measurements were performed in FEMR at McGill University, Montreal, Canada. The authors thank Kelly Sears, Liu David, and Jeannie Mui, for assistance with TEM.

References

[1] Y. Shen, Y. Lin, M. Li, and C.-W. Nan, "High dielectric performance of polymer composite films induced by a percolating interparticle barrier layer," *Advanced Materials*, vol. 19, no. 10, pp. 1418–1422, 2007.

[2] T. J. Lewis, "Interfaces are the dominant feature of dielectrics at the nanometric level," *IEEE Transactions on Dielectrics and Electrical Insulation*, vol. 11, no. 5, pp. 739–753, 2004.

[3] Y. Sun, Z. Zhang, and C. P. Wong, "Influence of interphase and moisture on the dielectric spectroscopy of epoxy/silica composites," *Polymer*, vol. 46, no. 7, pp. 2297–2305, 2005.

[4] E. Tuncer, A. J. Rondinone, J. Woodward, I. Sauers, D. R. James, and A. R. Ellis, "Cobalt iron-oxide nanoparticle modified poly(methyl methacrylate) nanodielectrics," *Applied Physics A: Materials Science and Processing*, vol. 94, no. 4, pp. 843–852, 2009.

[5] E. Tuncer, B. Nettelblad, and S. M. Gubañski, "Non-Debye dielectric relaxation in binary dielectric mixtures (50-50): randomness and regularity in mixture topology," *Journal of Applied Physics*, vol. 92, no. 8, pp. 4612–4624, 2002.

[6] A. A. Vorob'ev, "Excitation and electrical breakdown of solid insulators," *Soviet Physics Journal*, vol. 23, no. 5, pp. 382–386, 1980.

[7] J. Artbauer, "Electric strength of polymers," *Journal of Physics D: Applied Physics*, vol. 29, no. 2, pp. 446–456, 1996.

[8] N. Venkatasubramanian, K. J. Wiacek, S. Fries-Carr, E. Fossum, and T. D. Dang, "High-temperature polymer dielectrics for capacitive energy-storage applications," in *Proceedings of the 5th International Symposium on Polyimides and Other High Temperature Polymers*, p. 393, 2007.

[9] A. Schneuwly, P. Gröning, L. Schlapbach, C. Irrgang, and J. Vogt, "Breakdown behavior of oil-impregnated polypropylene as dielectric in film capacitors," *IEEE Transactions on Dielectrics and Electrical Insulation*, vol. 5, no. 6, pp. 862–868, 1998.

[10] I. L. Hosier, A. S. Vaughan, and S. G. Swingler, "The effects of measuring technique and sample preparation on the breakdown strength of polyethlyene," *IEEE Transactions on Dielectrics and Electrical Insulation*, vol. 9, no. 3, pp. 353–361, 2002.

[11] A. E. Job, N. Alves, M. Zanin et al., "Increasing the dielectric breakdown strength of poly(ethylene terephthalate) films using a coated polyaniline layer," *Journal of Physics D: Applied Physics*, vol. 36, no. 12, pp. 1414–1417, 2003.

[12] M. Ieda, "Dielectric breakdown process of polymers," *IEEE Transactions on Electrical Insulation*, vol. 15, no. 3, pp. 206–224, 1979.

[13] V. A. Zakrevskii, N. T. Sudar, A. Zaopo, and Y. A. Dubitsky, "Mechanism of electrical degradation and breakdown of insulating polymers," *Journal of Applied Physics*, vol. 93, no. 4, pp. 2135–2139, 2003.

[14] G. Chen and A. E. Davies, "The influence of defects on the short-term breakdown characteristics and long-term dc performance of LDPE insulation," *IEEE Transactions on Dielectrics and Electrical Insulation*, vol. 7, no. 3, pp. 401–407, 2000.

[15] T. J. Lewis, "Nanometric dielectrics," *IEEE Transactions on Dielectrics and Electrical Insulation*, vol. 1, no. 5, pp. 812–825, 1994.

[16] D. Ma, T. A. Hugener, R. W. Siegel et al., "Influence of nanoparticle surface modification on the electrical behaviour of polyethylene nanocomposites," *Nanotechnology*, vol. 16, no. 6, pp. 724–731, 2005.

[17] G. C. Montanari, D. Fabiani, F. Palmieri, D. Kaempfer, R. Thomann, and R. Mülhaupt, "Modification of electrical properties and performance of EVA and PP insulation through nanostructure by organophilic silicates," *IEEE Transactions on Dielectrics and Electrical Insulation*, vol. 11, no. 5, pp. 754–762, 2004.

[18] C. D. Green, A. S. Vaughan, G. R. Mitchell, and T. Liu, "Structure property relationships in polyethylene/montmorillonite nanodielectrics," *IEEE Transactions on Dielectrics and Electrical Insulation*, vol. 15, no. 1, pp. 134–143, 2008.

[19] M. Hoyos, N. García, R. Navarro et al., "Electrical strength in ramp voltage AC tests of LDPE and its nanocomposites with silica and fibrous and laminar silicates," *Journal of Polymer Science B: Polymer Physics*, vol. 46, no. 13, pp. 1301–1311, 2008.

[20] J. Gao, N. Guo, Y. Liu et al., "Effect of compound technology on polyethylene/ montmorillonite composites," in *Proceedings of the 9th IEEE International Conference on the Properties and Applications of Dielectric Materials (ICPADM '09)*, pp. 781–784, July 2009.

[21] V. Tomer, G. Polizos, C. A. Randall, and E. Manias, "Polyethylene nanocomposite dielectrics: implications of nanofiller orientation on high field properties and energy storage," *Journal of Applied Physics*, vol. 109, no. 7, Article ID 074113, 2011.

[22] G. Junguo, Z. Jinmei, J. Quanquan, L. Jiayin, Z. Mingyan, and Z. Xiaohong, "Study on brekdown and paitial discharge of polyethylene/montmorillonite nanocomposites," in *Proceedings of the International Symposium on Electrical Insulating Materials (ISEIM '08)*, pp. 597–600, September 2008.

[23] T. Tanaka, G. C. Montanari, and R. Mülhaupt, "Polymer nanocomposites as dielectrics and electrical insulation-perspectives for processing technologies, material characterization and future applications," *IEEE Transactions on Dielectrics and Electrical Insulation*, vol. 11, no. 5, pp. 763–784, 2004.

[24] E. David, M. Fréchette, B. Zazoum, C. Daran-Daneau, A. D. Ngô, and H. Couderc, "Dielectric properties of PE/clay nanocomposites," *Journal of Nanomaterials*, vol. 2013, Article ID 703940, 11 pages, 2013.

[25] A. Ranade, N. A. D'Souza, and B. Gnade, "Exfoliated and intercalated polyamide-imide nanocomposites with montmorillonite," *Polymer*, vol. 43, no. 13, pp. 3759–3766, 2002.

[26] J. Gaume, C. Taviot-Gueho, S. Cros, A. Rivaton, S. Thérias, and J.-L. Gardette, "Optimization of PVA clay nanocomposite for ultra-barrier multilayer encapsulation of organic solar cells," *Solar Energy Materials and Solar Cells*, vol. 99, pp. 240–249, 2012.

[27] S.-I. Hong and J.-W. Rhim, "Preparation and properties of melt-intercalated linear low density polyethylene/clay nanocomposite films prepared by blow extrusion," *LWT—Food Science and Technology*, vol. 48, no. 1, pp. 43–51, 2012.

[28] B. Zazoum, E. David, and A. Ngô, "LDPE/HDPE/clay nanocomposites: effects of compatibilizer on the structure and dielectric response," *Journal of Nanotechnology*, vol. 2013, Article ID 138457, 10 pages, 2013.

[29] J. Morawiec, A. Pawlak, M. Slouf, A. Galeski, E. Piorkowska, and N. Krasnikowa, "Preparation and properties of compatibilized LDPE/organo-modified montmorillonite nanocomposites," *European Polymer Journal*, vol. 41, no. 5, pp. 1115–1122, 2005.

[30] S. P. Lonkar, S. Therias, F. Leroux, J.-L. Gardette, and R. P. Singh, "Thermal, mechanical, and rheological characterization of polypropylene/layered double hydroxide nanocomposites," *Polymer Engineering & Science*, vol. 52, pp. 2006–2014, 2012.

[31] G. S. Venkatesh, A. Deb, A. Karmarkar, and S. S. Chauhan, "Effect of nanoclay content and compatibilizer on viscoelastic properties of montmorillonite/polypropylene nanocomposites," *Materials and Design*, vol. 37, pp. 285–291, 2012.

[32] R. A. Vaia, R. K. Teukolsky, and E. P. Giannelis, "Interlayer structure and molecular environment of alkylammonium layered silicates," *Chemistry of Materials*, vol. 6, no. 7, pp. 1017–1022, 1994.

[33] W. Lertwimolnun and B. Vergnes, "Influence of compatibilizer and processing conditions on the dispersion of nanoclay in a polypropylene matrix," *Polymer*, vol. 46, no. 10, pp. 3462–3471, 2005.

[34] J. K. Nelson and J. C. Fothergill, "Internal charge behaviour of nanocomposites," *Nanotechnology*, vol. 15, no. 5, pp. 586–595, 2004.

[35] M. Hoyos, N. García, R. Navarro et al., "Electrical strength in ramp voltage AC tests of LDPE and its nanocomposites with silica and fibrous and laminar silicates," *Journal of Polymer Science B: Polymer Physics*, vol. 46, no. 13, pp. 1301–1311, 2008.